nature materials

Supplementary information

https://doi.org/10.1038/s41563-026-02594-7

# Boundary geometry controls a topological defect transition that determines lumen nucleation in embryonic development

In the format provided by the authors and unedited

## CONTENTS



## SUPPLEMENTARY NOTES

### Supplementary Note 1: Minimisation of the free energy functional and derivation of the Euler-Lagrange equations

In order to find the value of the vector field $\mathbf{p}(\mathbf{r})$ that minimises the free energy functional

$$\mathcal{F}[\mathbf{p}] = \int_\Omega \mathrm{d}V f_{\mathrm{B}}(\mathbf{p}, \nabla\mathbf{p}) + \int_{\partial\Omega} \mathrm{d}S f_{\mathrm{S}}(\mathbf{p})\,, \tag{1}$$

in a volume $\Omega$, we write the variation

$$\delta\mathcal{F} = \int_\Omega \mathrm{d}V \left[\frac{\partial f_{\mathrm{B}}}{\partial p_i}\delta p_i + \frac{\partial f_{\mathrm{B}}}{\partial\left(\nabla p_i\right)}\cdot\nabla\left(\delta p_i\right)\right] + \int_{\partial\Omega}\mathrm{d}S\,\frac{\partial f_{\mathrm{S}}}{\partial p_i}\delta p_i\,, \tag{2}$$

where Einstein summation convention over repeated indexes is used. The second term of the volume integral can be integrated by parts to yield

$$\begin{aligned}\int_\Omega \mathrm{d}V \frac{\partial f_{\mathrm{B}}}{\partial\left(\nabla p_i\right)}\cdot\nabla\left(\delta p_i\right) &= \int_\Omega \mathrm{d}V\left\{-\nabla\cdot\left[\frac{\partial f_{\mathrm{B}}}{\partial\left(\nabla p_i\right)}\right]\delta p_i + \nabla\cdot\left[\frac{\partial f_{\mathrm{B}}}{\partial\left(\nabla p_i\right)}\delta p_i\right]\right\} \\ &= -\int_\Omega \mathrm{d}V\,\nabla\cdot\left[\frac{\partial f_{\mathrm{B}}}{\partial\left(\nabla p_i\right)}\right]\delta p_i + \int_{\partial\Omega}\mathrm{d}S\,\hat{\mathbf{n}}\cdot\frac{\partial f_{\mathrm{B}}}{\partial\left(\nabla p_i\right)}\delta p_i\end{aligned} \tag{3}$$

with $\hat{\mathbf{n}}$ the outward normal. Thus, equation (2) becomes

$$\delta\mathcal{F} = \int_\Omega \mathrm{d}V\left[\frac{\partial f_{\mathrm{B}}}{\partial p_i} - \nabla\cdot\frac{\partial f_{\mathrm{B}}}{\partial\left(\nabla p_i\right)}\right]\delta p_i + \int_{\partial\Omega}\mathrm{d}S\left[\frac{\partial f_{\mathrm{S}}}{\partial p_i} + \hat{\mathbf{n}}\cdot\frac{\partial f_{\mathrm{B}}}{\partial\left(\nabla p_i\right)}\right]\delta p_i\,. \tag{4}$$

If the minimising field $\mathbf{p}$ were to have a fixed value on the boundary (essential boundary conditions), $\delta p_i\big|_{\partial\Omega} = 0$ and the surface integral would vanish directly. In our case, however, we take boundary conditions on $\mathbf{p}$ to be natural, meaning that they are not imposed externally, but are *naturally* derived form the problem and satisfied after a solution has been found. Hence, for arbitrary variations $\delta p_i$, we enforce

$$\frac{\partial f_{\mathrm{S}}}{\partial p_i} + \hat{\mathbf{n}}\cdot\frac{\partial f_{\mathrm{B}}}{\partial\left(\nabla p_i\right)} = 0 \quad \text{in } \partial\Omega\,. \tag{5}$$

These equations ensure continuity of $\mathbf{p}$ on the surface and leave us only with the volume integral. Finally, asking that $\delta\mathcal{F} = 0$ gives rise to the set of coupled partial differential equations

$$\frac{\partial f_{\mathrm{B}}}{\partial p_i} - \nabla\cdot\frac{\partial f_{\mathrm{B}}}{\partial\left(\nabla p_i\right)} = 0 \quad \text{in } \Omega\,, \tag{6}$$

which are the Euler-Lagrange equations of the problem.

## Supplementary Note 2: Relation between the elastic contribution $f_{\mathrm{E}}$ and the Frank free energy density

The expression used in this work for the elastic energy density is

$$f_{\mathrm{E}} = \frac{k_0}{2}\left(\nabla\cdot\mathbf{p}\right)^2 + \frac{k_1}{2}[\hat{\mathbf{p}}\cdot(\nabla\times\mathbf{p})]^2 + \frac{k_2}{2}[\hat{\mathbf{p}}\times(\nabla\times\mathbf{p})]^2 . \tag{7}$$

In this section we discuss its relation to the more standard Frank free energy density.

### *In the one-constant approximation*

Typically [1–4], the elastic energy density of a vector field $\mathbf{p}$ is taken to be

$$f_{\mathrm{Frank}} = \frac{k}{2}(\partial_i p_j)(\partial_i p_j) \tag{8}$$

with $\partial_i \equiv \partial/\partial x_i$ and $k>0$ the Frank constant. Using explicitly that $\mathbf{p}=|\mathbf{p}|\hat{\mathbf{p}}$ and $\hat{p}_j\partial_i\hat{p}_j \propto \partial_i(\hat{p}_j\hat{p}_j)=\partial_i(1)=0$, it can be rewritten as

$$f_{\mathrm{Frank}} = \frac{k}{2}\left[(\nabla|\mathbf{p}|)^2 + |\mathbf{p}|^2(\partial_i\hat{p}_j)(\partial_i\hat{p}_j)\right] . \tag{9}$$

The last term can be decomposed into four terms corresponding to the splay, twist, bend and saddle-splay modes [5], thus giving rise to

$$f_{\mathrm{Frank}} = \frac{k}{2}\left\{(\nabla|\mathbf{p}|)^2 + |\mathbf{p}|^2\left[(\nabla\cdot\hat{\mathbf{p}})^2 + [\hat{\mathbf{p}}\cdot(\nabla\times\hat{\mathbf{p}})]^2 + [\hat{\mathbf{p}}\times(\nabla\times\hat{\mathbf{p}})]^2\right]\right\} + f_{\mathrm{saddle-splay}} \tag{10}$$

with $f_{\mathrm{saddle-splay}} = -k|\mathbf{p}|^2\nabla\cdot\left[\hat{\mathbf{p}}(\nabla\cdot\hat{\mathbf{p}}) + \hat{\mathbf{p}}\times(\nabla\times\hat{\mathbf{p}})\right]/2$.

Let us now consider the elastic energy density (7) with $k_0=k_1=k_2\equiv k$, that is,

$$f_{\mathrm{E}'} = \frac{k}{2}\left\{(\nabla\cdot\mathbf{p})^2 + [\hat{\mathbf{p}}\cdot(\nabla\times\mathbf{p})]^2 + [\hat{\mathbf{p}}\times(\nabla\times\mathbf{p})]^2\right\} . \tag{11}$$

Notice that the prime is used throughout this section to emphasise the one-constant approximation. We can expand each term as

$$(\nabla\cdot\mathbf{p})^2 = |\mathbf{p}|^2(\nabla\cdot\hat{\mathbf{p}})^2 + (\nabla|\mathbf{p}|\cdot\hat{\mathbf{p}})^2 + 2|\mathbf{p}|(\nabla|\mathbf{p}|\cdot\hat{\mathbf{p}})(\nabla\cdot\hat{\mathbf{p}}) \tag{12}$$

$$[\hat{\mathbf{p}}\cdot(\nabla\times\mathbf{p})]^2 = |\mathbf{p}|^2[\hat{\mathbf{p}}\cdot(\nabla\times\hat{\mathbf{p}})]^2 \tag{13}$$

$$[\hat{\mathbf{p}}\times(\nabla\times\mathbf{p})]^2 = |\mathbf{p}|^2[\hat{\mathbf{p}}\times(\nabla\times\hat{\mathbf{p}})]^2 + [\hat{\mathbf{p}}\times(\nabla|\mathbf{p}|\times\hat{\mathbf{p}})]^2 + 2|\mathbf{p}|\,[\hat{\mathbf{p}}\times(\nabla|\mathbf{p}|\times\hat{\mathbf{p}})]\cdot[\hat{\mathbf{p}}\times(\nabla\times\hat{\mathbf{p}})] \tag{14}$$

The first terms of each identity are equal to the the terms in square brackets in equation (10), and the sum of the second terms of identities (12) and (14) is equal to $(\nabla|\mathbf{p}|)^2$. The sum of their third terms, however, is not present in equation (10); we use it to write the cross-term energy density

$$f_{\mathrm{cross}'} = k\left\{(\mathbf{p}\cdot\nabla|\mathbf{p}|)(\nabla\cdot\hat{\mathbf{p}}) + [\mathbf{p}\times(\nabla|\mathbf{p}|\times\hat{\mathbf{p}})]\cdot[\hat{\mathbf{p}}\times(\nabla\times\hat{\mathbf{p}})]\right\} . \tag{15}$$

With this, we have that $f_{\mathrm{E}'} = f_{\mathrm{Frank}} - f_{\mathrm{saddle-splay}} + f_{\mathrm{cross}'}$.

We now evaluate numerically the difference between the standard Frank free energy density (8) and the approximated expression (11). We consider the free energy functional given by equation (1), and use $f_{\mathrm{B}} = f_{\mathrm{A}} + f_\eta$ with $f_{\mathrm{A}}$

as defined in the main text and $f_\eta$ a placeholder for $f_{\text{Frank}}$ or $f_{\text{E}'}$. The surface energy density $f_{\text{S}}$ is also taken to be the same as in the main text, with a mixed preferred orientation in the boundary. We minimise equation (1) in a sphere without assuming any symmetry to find the corresponding OP fields $\mathbf{p}_\eta$ (Supplementary Fig. 1a). In order to evaluate discrepancies in the results quantitatively, we define the relative energy difference

$$\Sigma \equiv \frac{H_{\text{Frank}} - H_{\text{E}'}}{H_{\text{Frank}}} \,, \tag{16}$$

where $H_\eta$ is the total energy of the system with OP $\mathbf{p}_\eta$ and elastic energy density $f_\eta$, and the average difference between the OP fields

$$\Pi \equiv \frac{1}{N_{\text{s}}} \sum_{i=1}^{N_{\text{s}}} |\mathbf{p}_{\text{Frank}}(\mathbf{r}_i) - \mathbf{p}_{\text{E}'}(\mathbf{r}_i)| \,, \tag{17}$$

where $N_{\text{s}}$ is the number of nodes in the mesh. Both $\Sigma$ and $\Pi$ show that $\mathbf{p}_{\text{Frank}}$ and $\mathbf{p}_{\text{E}'}$ present excellent agreement in the low $\zeta = \xi^2/\lambda$ regime (Supplementary Figs. 1b-c). Note that both fields present a radial boojum on the top cap like that of Fig. 1c (bottom line, second leftmost panel) in the main text. Conversely, differences between $\mathbf{p}_{\text{Frank}}$ and $\mathbf{p}_{\text{E}'}$ are most significant in the high $\zeta$ regime. Nonetheless, both OP fields are topologically equivalent to each other and to the uniform field.

*Leaving the one-constant approximation*

We now focus on the elastic energy density of equation (7) in the splay-dominated regime ($k_0 \gg k_2$). Minimisation of equation (1) in the full 3D, symmetry-agnostic case leads to an OP field consisting on a positive hyperbolic hedgehog on the $z$ axis and a radial disclination ring around it (Supplementary Fig. 2a). This supports the assumption of axial symmetry made in the main text (Supplementary Fig. 2b), and rules out the possibility of spontaneous selection of a given value of the azimuth angle $\phi$ for an off-axis point defect instead of the ring.

In this more general case, the cross-term energy density is given by

$$f_{\text{cross}} = k_0(\mathbf{p} \cdot \nabla|\mathbf{p}|)(\nabla \cdot \hat{\mathbf{p}}) + k_2 \left[\mathbf{p} \times (\nabla|\mathbf{p}| \times \hat{\mathbf{p}})\right] \cdot \left[\hat{\mathbf{p}} \times (\nabla \times \hat{\mathbf{p}})\right] . \tag{18}$$

We use this expression to define the error score

$$\epsilon \equiv \frac{H_{\text{cross}}}{H_{\text{E}}} \,, \tag{19}$$

where $H_{\text{cross}} = \int_\Omega \mathrm{d}V f_{\text{cross}}$. This value is a proxy for the previous relative energy difference and average OP difference, which allows us to approximately evaluate the discrepancy between the numerical results using equation (7) and the corresponding Frank free energy density, without having to compute the latter. Supplementary Fig. 3 present the error score of the results depicted in the main text.

## SUPPLEMENTARY FIGURES

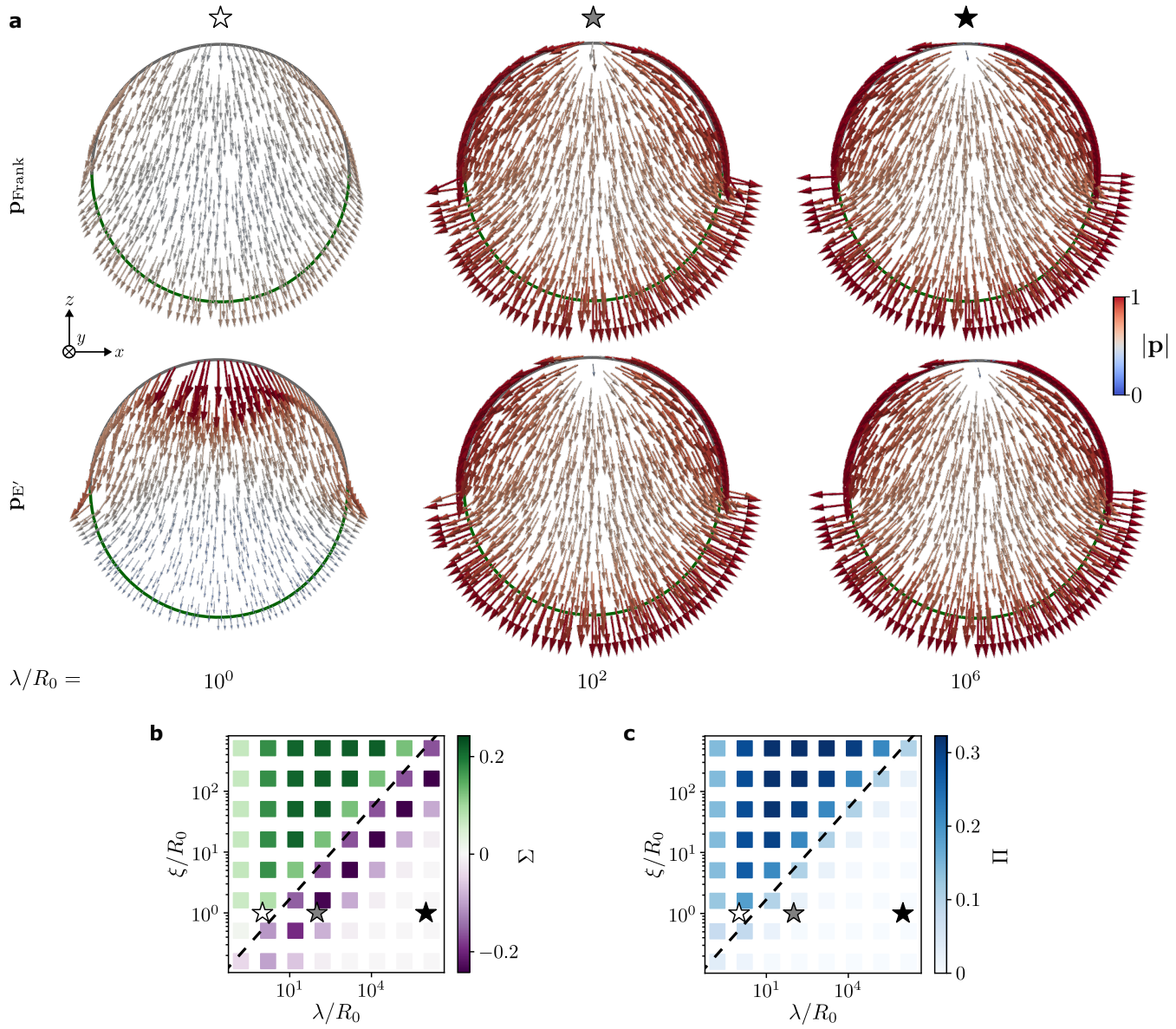


Supplementary Figure 1. **Numerical evaluation of the difference between the standard Frank free energy density and the elastic energy terms in the one-constant approximation. a,** Central slices of the 3D OP-field configurations obtained using $f_{\mathrm{Frank}}$ and $f_{\mathrm{E}'}$ in a sphere for $\xi/R_0 = 1$ and different values of $\lambda/R_0 = 10$. Colour map and arrow size encode the magnitude of the OP. **b-c,** Relative energy difference [**b**, equation (16)] and average OP difference [**c**, equation (17)] vs. $\lambda/R_0$ and $\xi/R_0$ in spherical confinement. Both quantities indicate an excellent agreement of the results for small values of $\zeta$. As a reference, the dashed line shows the value $\zeta^* \approx 0.3R_0$ of the main text. Stars highlight the sets of parameters where the configurations of panel **a** were obtained.

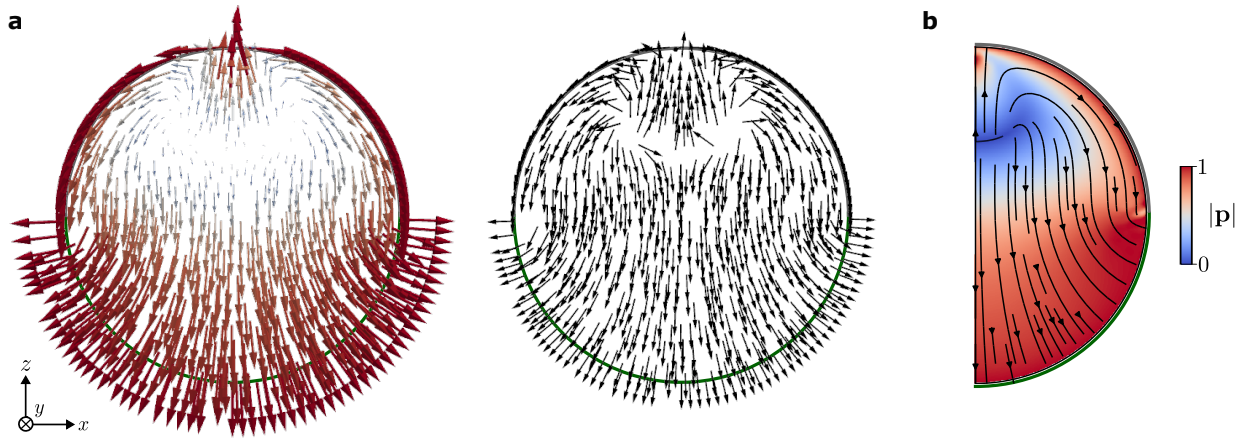


Supplementary Figure 2. **3D solution consists of a positive hyperbolic hedgehog and a radial disclination ring. a,** Central slice of the 3D OP field obtained with $f_{\mathrm{E}}$ in the splay-dominated regime and spherical confinement ($\lambda/R_0 = 10^6$, $\xi/R_0 = 1$, $k_0/k_2 = 10$). Colour map and arrow size encode the magnitude of the OP (left). For clarity, a normalised, rescaled version of the OP is also shown (right). **b,** The same configuration is obtained in the main work when the assumption of axial symmetry is made. Streamlines and colour map depict the field direction and magnitude, respectively.

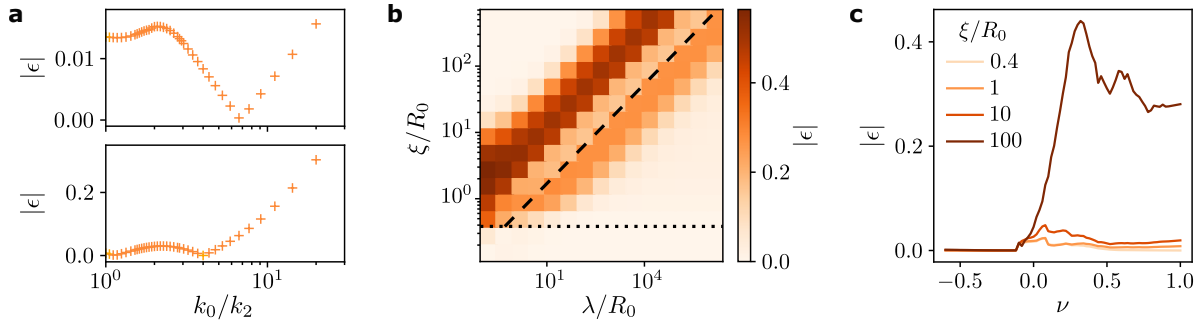


Supplementary Figure 3. **Error score [equation (19)] for the results in the main text. a,** Error score as a function of $k_0/k_2$ for longitudinal parallel (upper panel) and mixed (lower panel) preferred orientations in spherical confinement ($\lambda/R_0 = 100$, $\xi/R_0 = 1$). **b,** Error score vs. $\lambda/R_0$ and $\xi/R_0$ in spherical confinement with mixed $\mathbf{p}_0$ in the splay-dominated regime ($k_0/k_2 = 10$). **c,** Error score as a function of the acorn parameter $\nu$ for different values of $\xi/R_0$ ($\lambda/R_0 = 10^6$, $k_0/k_2 = 10$).

## SUPPLEMENTARY REFERENCES


[1] P.-G. De Gennes and J. Prost, *The physics of liquid crystals*, 2nd ed., 83 (Oxford University Press, New York, 1993).

[2] R. Alert, C. Blanch-Mercader, and J. Casademunt, Physical Review Letters **122**, 088104 (2019).

[3] M. E. Pallarès, I. Pi-Jaumà, I. C. Fortunato, V. Grazu, M. Gómez-González, P. Roca-Cusachs, J. M. de la Fuente, R. Alert, R. Sunyer, J. Casademunt, *et al.*, Nature Physics **19**, 279 (2023).

[4] M. Ibrahimi and M. Merkel, New Journal of Physics **25**, 013022 (2023).

[5] J. V. Selinger, Liquid Crystals Reviews **6**, 129 (2018).